



Characterization of the Methanomicrobial Archaeal RNase Zs for Processing the CCA-Containing tRNA Precursors

Xiaoyan Wang^{1,2†}, Xien Gu^{1†}, Jie Li^{3*†}, Lei Yue^{3,4}, Defeng Li³ and Xiuzhu Dong^{3,4*}

¹ Department of Biochemistry and Molecular Biology, Institute of Basic Medical Sciences, College of Basic Medicine, Hubei University of Medicine, Shiyan, China, ² Hubei Key Laboratory of Embryonic Stem Cell Research, Hubei University of Medicine, Shiyan, China, ³ State Key Laboratory of Microbial Resources, Institute of Microbiology, Chinese Academy of Sciences, Beijing, China, ⁴ State Key Laboratory of Microbial Resources, University of Chinese Academy of Sciences, Beijing, China

OPEN ACCESS

Edited by:

Fengping Wang,
Shanghai Jiao Tong University, China

Reviewed by:

Changyi Zhang,
University of Illinois at
Urbana–Champaign, United States
Xi-Peng Liu,
Shanghai Jiao Tong University, China

*Correspondence:

Jie Li
lijie824@im.ac.cn
Xiuzhu Dong
dongxz@im.ac.cn

†These authors have contributed
equally to this work

Specialty section:

This article was submitted to
Biology of Archaea,
a section of the journal
Frontiers in Microbiology

Received: 10 February 2020

Accepted: 15 July 2020

Published: 25 August 2020

Citation:

Wang X, Gu X, Li J, Yue L, Li D
and Dong X (2020) Characterization
of the Methanomicrobial Archaeal
RNase Zs for Processing
the CCA-Containing tRNA Precursors.
Front. Microbiol. 11:1851.
doi: 10.3389/fmicb.2020.01851

RNase Z is a widely distributed and usually essential endoribonuclease involved in the 3'-end maturation of transfer RNAs (tRNAs). A CCA triplet that is needed for tRNA aminoacylation in protein translation is added by a nucleotidyl-transferase after the 3'-end processing by RNase Z. However, a considerable proportion of the archaeal pre-tRNAs genetically encode a CCA motif, while the enzymatic characteristics of the archaeal RNase (aRNase) Zs in processing CCA-containing pre-tRNAs remain unclear. This study intensively characterized two methanomicrobial aRNase Zs, the *Methanobrevibacter smithii* mpy-RNase Z and the *Methanococcus maripaludis* mmp-RNase Z, particularly focusing on the properties of processing the CCA-containing pre-tRNAs, and in parallel comparison with a bacterial bsu-RNase Z from *Bacillus subtilis*. Kinetic analysis found that Co²⁺ supplementation enhanced the cleavage efficiency of mpy-RNase Z, mmp-RNase Z, and bsu-RNase Z for 1400-, 2990-, and 34-fold, respectively, and Co²⁺ is even more indispensable to the aRNase Zs than to bsu-RNase Z. Mg²⁺ also elevated the initial cleavage velocity (V₀) of bsu-RNase Z for 60.5-fold. The two aRNase Zs exhibited indiscriminate efficiencies in processing CCA-containing vs. CCA-less pre-tRNAs. However, V₀ of bsu-RNase Z was markedly reduced for 1520-fold by the CCA motif present in pre-tRNAs under Mg²⁺ supplementation, but only 5.8-fold reduced under Co²⁺ supplementation, suggesting Co²⁺ could ameliorate the CCA motif inhibition on bsu-RNase Z. By 3'-RACE, we determined that the aRNase Zs cleaved just downstream the discriminator nucleotide and the CCA triplet in CCA-less and CCA-containing pre-tRNAs, thus exposing the 3'-end for linking CCA and the genetically encoded CCA triplet, respectively. The aRNase Zs, but not bsu-RNase Z, were also able to process the intron-embedded archaeal pre-tRNAs, and even process pre-tRNAs that lack the D, T, or anticodon arm, but strictly required the acceptor stem. In summary, the two methanomicrobial aRNase Zs use cobalt as a metal ligand and process a broad spectrum of pre-tRNAs, and the characteristics would extend our understandings on aRNase Zs.

Keywords: aRNase Z, precursor tRNA, 3' end processing, tRNA maturation, CCA motif, methanomicrobial archaea

INTRODUCTION

Transfer RNAs (tRNAs) carry specific amino acids to ribosome and decode messenger RNAs (mRNAs) through base-pairing between the anticodon sequence in tRNA and the corresponding codon in mRNA, and thus play a pivotal role in protein translation (Redko et al., 2007; Kirchner and Ignatova, 2015). All tRNAs are transcribed as precursors that have to be processed to the mature functional form. Maturation of tRNA precursors (pre-tRNAs) is accomplished through several processing steps, including removal of the 5'-leader and 3'-trailer sequences, excision of introns in eukaryotic and some archaeal pre-tRNAs, nucleotide modifications, and the addition of a CCA triplet at the 3'-end (Redko et al., 2007). The endoribonuclease RNase P performs the 5'-end processing (Guerriertakada et al., 1983; Holzmann et al., 2008), while the endoribonuclease RNase Z plays an essential role in removal of the 3'-trailer from pre-tRNAs, and the CCA triplet that is needed for tRNA aminoacylation is added by a nucleotidyl-transferase after the 3'-end processing by RNase Z (Cudny and Deutscher, 1986; Cudny et al., 1986).

The tRNA 3'-end maturation through an endoribonucleolytic processing was first discovered in eukaryotes (Nashimoto, 1997; Kunzmann et al., 1998; Mohan et al., 1999; Schiffer et al., 2001). The functional endoribonuclease, RNase Z, was first purified as a homogeneous protein from *Arabidopsis thaliana* (Schiffer et al., 2002), and then its orthologs have been widely characterized among bacteria (Pellegrini et al., 2003; Minagawa et al., 2004; Ceballos-Chavez and Vioque, 2005; Ezraty et al., 2005; Dutta and Deutscher, 2009), and some halophilic and thermophilic euryarchaea (Schierling et al., 2002; Spaeth et al., 2008). These investigations have demonstrated that RNase Z endonucleolytically hydrolyzes the phosphodiester bond directly downstream of the discriminator nucleotide, an unpaired nucleotide at the 3'-end of the acceptor stem, thus resulting in a processed tRNA with a 3'-hydroxyl group. These studies also found that the nucleotide type of the discriminator does not affect but cytidines present directly downstream it severely suppress the 3'-trailer removal efficiency of RNase Z. The *Bacillus subtilis*, and wheat RNase Zs, all poorly cleave a 3'-trailer sequence beginning with CC, CCA, or CCA with one or two extra nucleotides. So the CCA motif in pre-tRNA 3'-end has been identified as a general repressor of RNase Zs (Mohan et al., 1999; Pellegrini et al., 2003). Different from the eukaryotic tRNA genes, which do not encode the CCA motif in general, the archaeal and bacterial tRNA genes, with varying proportions, encode the CCA motif (Redko et al., 2007). Therefore, in bacteria, a different processing pathway, which involves concerted actions of the endoribonuclease RNase E and a handful of exonucleases, is employed to trim the 3' extension downstream of the encoded CCA end (Li and Deutscher, 1996, 2002; Ow and Kushner, 2002; Wen et al., 2005). In some cases, RNase E cleavage directly generates the mature CCA terminus (Mohanty et al., 2016).

However, not all RNase Zs are generally inhibited by the CCA motif, such as the *Thermotoga maritima* RNase Z cleaves just downstream the CCA triplets in 45 tRNAs that carry the genetically encoded CCA (Minagawa et al., 2004), indicating that it could process the 3'-end of CCA-containing pre-tRNAs

in one step. Moreover, the *Escherichia coli* RNase Z, previously misidentified as RNase BN, is able to remove the 3'-end of pre-tRNAs ending as CA, CU, CCU, or even CCA (Asha et al., 1983). Additionally, a mammalian RNase Z also exhibits a measurable activity of cleaving downstream the CCA motif (Nashimoto, 1997). However, whether aRNase Zs process the CCA-containing pre-tRNAs as CCA-less ones have not been thoroughly elucidated.

RNase Z belongs to the family of metal-dependent β -lactamases, a group of metalloproteins that possess a conserved structural β -lactamase domain but with highly divergent sequences and functions (Callebaut et al., 2002). The protein structures of RNase Zs from *B. subtilis* (Li de la Sierra-Gallay et al., 2005, 2006), *T. maritima* (Ishii et al., 2005), and *E. coli* (Kostecky et al., 2006) all reveal a dimer of Zn^{2+} -containing metallo- β -lactamase domains with a protruded flexible arm that involves in tRNA binding. However, although two Zn^{2+} ions were observed in the catalytic center of the bacterial RNase (bRNase) Zs (Ishii et al., 2005; Li de la Sierra-Gallay et al., 2005), addition of Zn^{2+} did not, but Co^{2+} elevated the activity of *E. coli* RNase Z (Asha et al., 1983). Moreover, Mn^{2+} also stimulates the 3'-end processing activity of RNase Zs from *T. maritima* (Minagawa et al., 2006), *A. thaliana* (Spath et al., 2007), *Haloferax volcanii*, and *Pyrococcus furiosus* (Spaeth et al., 2008). Mn^{2+} amendment even rescues the lost Mg^{2+} -dependent activity of the *T. maritima* RNase Z catalytic mutants (Minagawa et al., 2006).

Methanomicrobial archaea are the most cultured and the most widely distributed archaeal representatives. They belong to the superphylum Euryarchaeota, one of the four major archaeal superphyla (Eme et al., 2017; Evans et al., 2019). However, the methanomicrobial aRNase Zs have not been intensively characterized. In this work, the *Methanobolus psychrophilus* mpy-RNase Z and *Methanococcus maripaludis* mmp-RNase Z were thoroughly investigated for the 3'-end processing activities in parallel comparison with a bRNase Z from *B. subtilis*, particularly focusing on the properties of processing CCA-containing pre-tRNAs. We found that Co^{2+} dramatically enhanced the catalytic efficiencies of both the archaeal and bRNase Zs for 1400-, 2990-, and 34-fold, respectively, and Co^{2+} appeared to be indispensable to the two aRNase Zs. The two methanomicrobial aRNase Zs indiscriminately processed CCA-containing and CCA-less pre-tRNAs, but CCA-motif severely suppressed the initial velocity of bRNase Z for 1520-fold unless Co^{2+} supplementation. Moreover, the two aRNase Zs were capable of processing the intron-containing pre-tRNAs and the aberrant pre-tRNA that contains only the acceptor stem, but required a mature 5'-end for the 3'-end processing and regardless of the 3' trailer lengths.

MATERIALS AND METHODS

Strains, Culture Conditions, and Genomic DNA Extraction

Methanococcus maripaludis S2 and *M. psychrophilus* R15 were, respectively, grown in pre-reduced McF medium at 37°C (Sarmiento et al., 2011) and a defined mineral medium

containing 20 mM trimethylamine at 18°C (Qi et al., 2017), and under a gas phase of N₂/CO₂ (80:20 v/v, 0.1 MPa). *E. coli* DH5 α , Rosetta (DE3), and *B. subtilis* 168 were grown at 37°C in Luria–Bertani (LB) broth supplemented with ampicillin (100 μ g/ml) or kanamycin (50 μ g/ml) when required.

The genomic DNA of *M. psychrophilus* R15, *M. maripaludis* S2, and *B. subtilis* 168 was extracted and purified from the mid-exponential cultures using the TIANamp Bacteria DNA Kit (TIANGEN Biotech, Beijing, China) by following the manufacturer's protocol. Purified DNA was quantified using a NanoPhotometer spectrophotometer (IMPLEN, Westlake Village, CA, United States), and DNA quality was checked by 2% agarose gel electrophoresis.

Cloning and Protein Expression

The open reading frames *Mpsy_2804* encoding mpy-RNase Z, *mmp0906* encoding mmp-RNase Z, and *bsu23840* encoding bsu-RNase Z were amplified by polymerase chain reaction (PCR) using the respective genomic DNAs and cloned between the *Nco*I site and the His tag encoding site of plasmid pET28a (Novagen) *via* stepwise Gibson assembly using the ClonExpress MultiS One Step Cloning Kit (Vazyme). The expression plasmids produce recombinant protein with a C-terminal His₆ tag. All cloned DNA sequences were verified by DNA sequencing, and the expression plasmids were transformed into *E. coli* Rosetta (DE3) competent cells. Transformants were cultured at 37°C in LB containing 50 μ g·ml⁻¹ kanamycin until OD₆₀₀ at 0.6–0.8, followed by 16 h of induction with 0.1 mM isopropyl- β -D-thiogalactoside at 22°C. Cells were harvested by centrifugation at 5000 \times *g* for 30 min at 4°C and then stored at –80°C until further analysis.

Protein Purification

The three RNase Zs – mpy-RNase Z, mmp-RNase Z, and bsu-RNase Z – were purified using a similar method as previously described (Zheng et al., 2017). The harvested cells were resuspended in binding buffer [20 mM HEPES pH 7.5, 500 mM NaCl, 20 mM imidazole, and 5% (w/v) glycerol], lysed by sonication, and centrifuged at 10,000 \times *g* for 60 min at 4°C. Then, supernatant was loaded on a HisTrap HP column (GE Healthcare) equilibrated with binding buffer and eluted with a linear gradient from 50 to 500 mM imidazole. The eluted protein was then dialyzed against buffer A [20 mM HEPES pH 7.5, 25 mM NaCl, 0.1 mM EDTA, and 5% (w/v) glycerol], loaded onto a HiTrap Q HP column (GE Healthcare), and eluted with a linear gradient of 100 mM to 1 M NaCl to remove the contaminative RNA and proteins. The eluted protein was validated to be RNA-free via measurement of the OD₂₆₀ to OD₂₈₀ ratio by a NanoDrop 2000 UV-Vis spectrophotometer (Thermo). Proteins with an OD₂₆₀ to OD₂₈₀ ratio below 0.6 were considered RNA-/DNA-free (Niedner et al., 2013). Finally, the purity of the RNA-free proteins was determined by SDS-PAGE, and the homogeneous protein was dialyzed against buffer B [20 mM HEPES pH 7.5, 150 mM NaCl, 5% (w/v) glycerol], concentrated using Amicon Ultrafra -30 concentrators (Millipore), flash-frozen, and stored at –80°C for biochemical assays. Protein concentration was determined using the Pierce BCA protein assay kit (Thermo Scientific).

In vitro Transcription of Pre-tRNA Substrates

Through *in vitro* transcription using the forward primer containing a T7 RNA polymerase promoter sequence (Supplementary Table S1), the pre-tRNA substrates (Supplementary Table S2) were prepared. The DNA templates of pre-tRNA^{mpy-Arg1} and its variants that carry varying lengths of 5' or 3' extensions, pre-tRNA^{mpy-Arg2(CCA)}, pre-tRNA^{mpy-Arg3(intron)}, and pre-tRNA^{mpy-Tyr(intron)} were prepared by PCR amplification from the genomic DNA of *M. psychrophilus* R15 using the corresponding primer pairs (Supplementary Table S1). The templates of pre-tRNA^{mmp-Arg1} and its variants carrying varying lengths of 5' or 3' extensions, pre-tRNA^{mmp-Arg2(CCA)}, pre-tRNA^{bsu-trnI}, pre-tRNA^{bsu-trnB(CCA)}, and pre-tRNA^{bsu-trn62(CCA)} were all prepared similarly. While the templates of pre-tRNA^{mpy-Arg1} and pre-tRNA^{mmp-Arg1} variants missing one mature tRNA part, either the D arm, anticodon arm, T arm, or acceptor stem, were synthesized by Sangon Biotech (Shanghai, China). Sequences of the pre-tRNAs used in this study are all listed in Supplementary Table S2. The amplified DNA templates were purified with a Wizard Gel and PCR Clean-UP System (Promega).

Next, the pre-tRNA substrates were produced by *in vitro* transcription as described previously (Zheng et al., 2017). *In vitro* transcriptions were conducted using the MEGAshortscript T7 Kit (Ambion) according to the manufacturer's instructions, and the transcribed RNA products were further purified by 10% denatured PAGE containing 8 M urea using the ZR small-RNA TMPAGE Recovery Kit (ZYMO) and then quantified with a NanoPhotometer spectrophotometer (IMPLEN, Westlake Village, CA, United States).

Nuclease Assays of RNase Zs

RNase Z activity was assayed in a 10 μ l reaction mixture in 20 mM HEPES pH 7.5, 150 mM NaCl, and 5% glycerol in the absence or presence of 1 mM ZnCl₂, CuCl₂, MgCl₂, or CoCl₂, and incubated at 37°C for 30 min or indicated time. Generally, 1.4 pmol pre-tRNA was used in all assays, and the protein concentration is indicated in each figure or figure legend. Reactions were initiated by the addition of enzyme, incubated at 37°C for 5–45 min, and stopped by incubation with 0.5 μ g/ml Proteinase K (Ambion) at 55°C for 15 min. After incubation, the reaction mixtures were mixed with formamide-containing dye (98% formamide, 5 mM EDTA, 0.025% bromophenol blue, 0.025% xylene cyanol, 0.025% SDS) and analyzed by 10% PAGE with 8 M urea. Oligoribonucleotides in lengths of 50, 80, and 169 nt were used as a molecular ladder to indicate the migration positions for RNA substrates and products. The urea-PAGE gels were stained by SYBR Gold for 10 min and then analyzed by fluorescence imaging with a Bio-Rad Gel doc XR+ (BIO-Rad).

Kinetic parameters of the three RNase Zs were determined by replicative quantification of the cleaving rate on various amounts (0.025–1 μ M) of the CCA-less and CCA-containing pre-tRNAs under different conditions listed in Table 1 and

TABLE 1 | Kinetic parameters of mpy-, mmp-, and bsu-RNase Zs for pre-tRNA 3'-end processing.

| Protein | Substrate | CoCl ₂ | K _m (μM) | k _{cat} (min ⁻¹) | k _{cat} /K _m (μM ⁻¹ min ⁻¹) |
|-------------|-------------------------------------|-------------------|------------------------|--|---|
| mpy-RNase Z | Pre-tRNA ^{mpy} -Arg1 | – | 0.6 | 0.0143 | 0.024 |
| | Pre-tRNA ^{mpy} -Arg1 | + | 0.26 | 8.7 | 33.46 |
| | Pre-tRNA ^{mpy} -Arg2(CCA) | + | 0.43 | 12 | 27.91 |
| mmp-RNase Z | Pre-tRNA ^{mmp} -Arg1 | – | 0.809 | 0.0045 | 0.0056 |
| | Pre-tRNA ^{mmp} -Arg1 | + | 0.36 | 6.3 | 17.5 |
| | Pre-tRNA ^{mmp} -Arg2(CCA) | + | 0.25 | 13.5 | 54 |
| bsu-RNase Z | Pre-tRNA ^{bsu} -trnI | – | 0.87 | 0.84 | 0.957 |
| | Pre-tRNA ^{bsu} -trnI | + | 0.89 | 28.8 | 32.36 |
| | Pre-tRNA ^{bsu} -trn62(CCA) | + | 0.56 | 1.4 | 2.5 |

A range of (0.025–1 μM) the genetically encoded CCA-lacking and CCA-containing pre-tRNA substrate concentrations were assayed for each tested RNase Z at 37°C in the absence (–) or presence (+) of 1 mM CoCl₂. Initial velocity (V₀) of RNase Z at each substrate concentration was determined through quantifying the substrate residuals in the linear phase during the initial 5 min similarly as that shown in **Figure 3**. The Lineweaver–Burk plots of the three RNase Zs for each substrate were shown in **Supplementary Figure S4**. The kinetic parameters of K_m, V_{max}, and k_{cat} were obtained by fitting the data to the Michaelis-Menten equation. Each set of values was from the averages of three replicates with a standard deviation of 3–15%.

Supplementary Figure S4. The reactions were performed at 37°C and the initial velocity (V₀) was determined through quantifying the substrate residuals in the linear phase during the initial 5 min as that shown in **Figure 3**. The substrate residual contents were rigorously quantified using the Quantity One software for three independent quantifications of the non-overexposure gels, and the confidential sampling points were used in V₀ and the Lineweaver–Burk plotting calculation. The Lineweaver–Burk plots of the three RNase Zs for each substrate are shown in **Supplementary Figure S4**. The kinetic parameters of K_m, V_{max}, and k_{cat} were obtained by fitting the data to the Michaelis-Menten equation.

Mapping of RNase Z Cleavage Sites

The cleavage sites in the CCA-less pre-tRNA^{mmp}-Arg1 and CCA-containing pre-tRNA^{mmp}-Arg2(CCA) generated by the three RNase Zs were mapped by rapid amplification of cDNA 3'-ends (3'-RACE). The primary cleaved products were first spliced from 10% urea-PAGE, recovered, and purified using the ZR small-RNA PAGE Recovery Kit (ZYMO) and quantified with a NanoPhotometer spectrophotometer (IMPLEN, Westlake Village, CA, United States). 3'-RACE was performed as described previously (Zhang et al., 2009). Briefly, total RNA (10 μg) was ligated with 50 pmol 3'-adaptor linker (5'-(rApp)CTGTAGGCACCATCAAT-NH₂-3'; NEB) through a 16 h incubation at 16°C with 20 U T4 RNA ligase (Ambion); 3' linker-ligated RNA was recovered by isopropanol precipitation, and one aliquot of 4 μg was mixed with 100 pmol 3'-R-RT-P (5'-ATTGATGGTGCCTACA G-3', complementary to the 3' RNA linker) by incubation

at 65°C for 10 min and on ice for 2 min. This sample was used in the reverse transcription (RT) reaction using 200 U of SuperScript III reverse transcriptase (Invitrogen). After RT, gene-specific PCR was conducted using primers (**Supplementary Table S1**) complementary to the 5'-end of pre-tRNAs to obtain specific products. Specific PCR products were excised from a 2% agarose gel, cloned into pMD19-T (TaKaRa), and sequenced. The 3'-ends of the RNase Z cleavage products were defined as the nucleotide linked to the 3'-RACE linker.

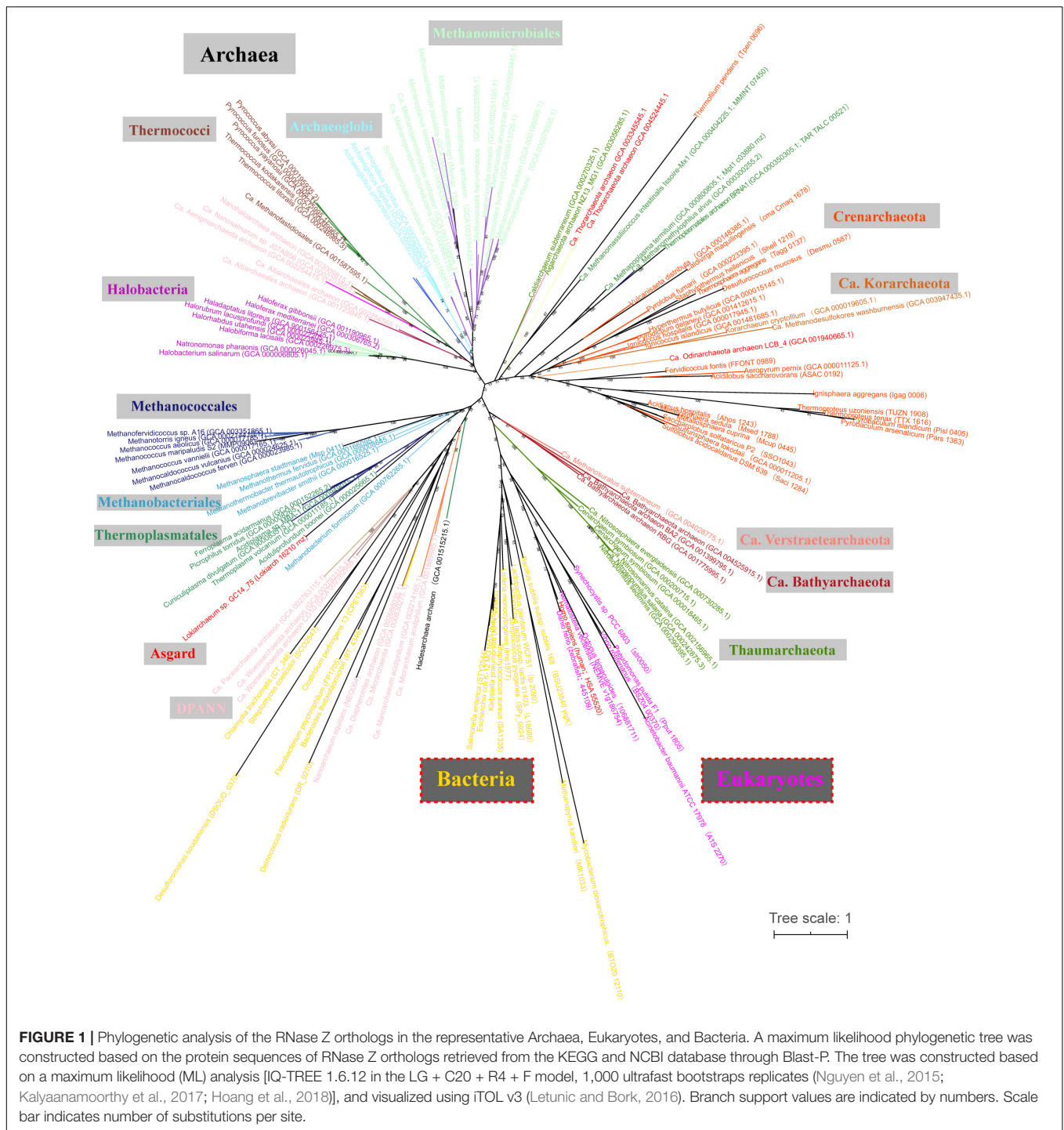
RESULTS

RNase Z Orthologs Are Widely Distributed in Archaea

Through a homolog search, RNase Z orthologs were found in most sequenced archaeal and eukaryotic genomes but not found in half of the searched bacterial genomes and particularly poorly represented in the phylum of Proteobacteria (**Supplementary Dataset S1**). Phylogenetically, most RNase Z orthologs were congruently clustered as the phylogenetic clades of archaeal species (**Figure 1**), implying that they could be vertically inherited in Archaea. Noticeably, RNase Z orthologs were found in all searched methanomicrobial archaeal genomes, including the 7th order (**Supplementary Dataset S1** and **Figure 1**), indicating that this protein could be essential to the methanomicrobial archaea. Therefore, two methanomicrobial aRNase Zs, mpy-RNase Z from *M. psychrophilus* that affiliates with the order of *Methanosarcinales* and mmp-RNase Z from *M. maripaludis* that belongs to *Methanococcales*, were chosen for investigation. The two proteins shared 38% amino-acid sequence identity (**Supplementary Figure S1**), and they were overexpressed in *E. coli* and purified as homogeneous proteins (**Supplementary Figure S2**). For comparison, a bRNase Z from *B. subtilis*, bsu-RNase Z, was purified and studied in parallel.

Co²⁺ Enhances the 3'-End Processing Activity of Both the Archaeal and Bacterial RNase Zs

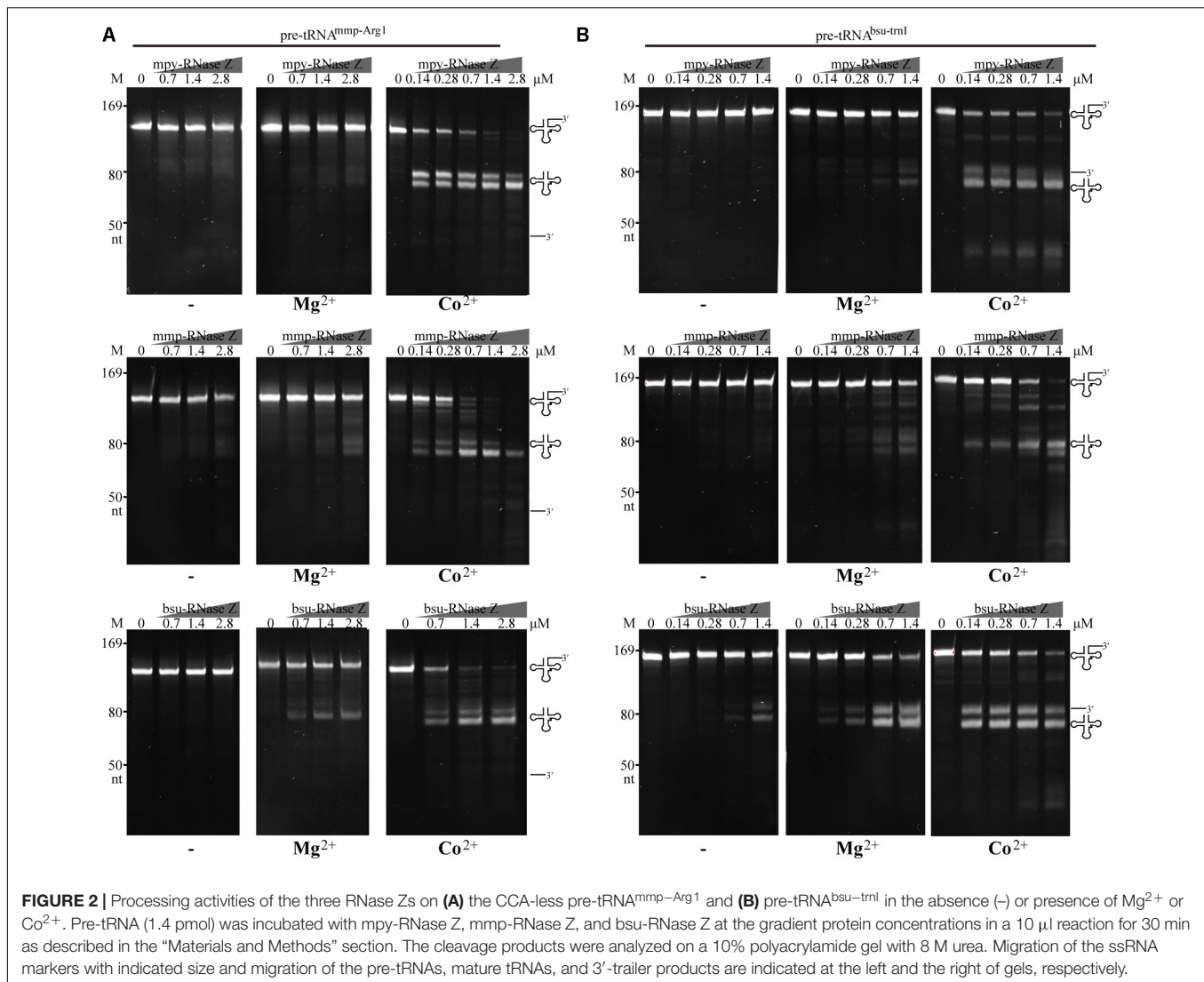
Archaeal RNase (aRNase) Zs affiliate with the β-lactamase family; therefore, the metal ions in facilitating the 3'-end processing activity were first examined. The *in vitro* transcribed bacterial pre-tRNA^{bsu}-trnI and archaeal pre-tRNA^{mmp}-Arg1 that carry an 83 nt and a 50 nt 3'-trailer, respectively, (**Supplementary Figures S3A,B**) were used as substrates. The recombinant mpy-RNase Z and mmp-RNase Z were incubated with each of the synthetic pre-tRNAs in a mixture supplemented with 1 mM of Co²⁺, or Mg²⁺ or Zn²⁺ or Cu²⁺. The bacterial bsu-RNase Z was assayed in parallel. Enzymatic assay determined that in Co²⁺ supplemented reactions, the three RNase Zs invariably cleaved 50–90% of the synthetic pre-tRNAs to generate abundant mature tRNAs (**Supplementary Figure S3**), while in Mg²⁺ amended reactions generated lower amounts of mature tRNA. These indicated that Co²⁺ enhances the 3'-end processing activity of the three RNase Zs, while Mg²⁺ has a weaker effect.



Neither Zn^{2+} nor Cu^{2+} enhanced the activities of the three RNase Zs, and even smear products occurred in the Zn^{2+} -supplemented reactions (**Supplementary Figure S3**), which could be presumably due to Zn^{2+} caused protein precipitation.

Stimulations of Co^{2+} and Mg^{2+} on RNase Zs' activities were then evaluated on processing the pre-tRNA^{mmp}-Arg¹ (**Figure 2A**) and pre-tRNA^{bsu}-trnI (**Figure 2B**) at gradient protein to RNA ratios of 20:1, 5:1, and 1:1. Enzymatic assays determined that

when Co^{2+} amended, at as low as 1:1 of protein to RNA, mature tRNAs generated by the two aRNase Zs were increased for ~30-fold, while when Mg^{2+} supplemented, mature tRNAs were increased for only ~two-fold than the reactions without metal-ion (**Figures 2A,B**, Co^{2+} , Mg^{2+} and -). While Co^{2+} showed similar enhancement on bsu-RNase Z, but Mg^{2+} showed stronger stimulation for 5–10-fold more mature tRNAs generated in the Mg^{2+} -amended reactions of bsu-RNase Z.



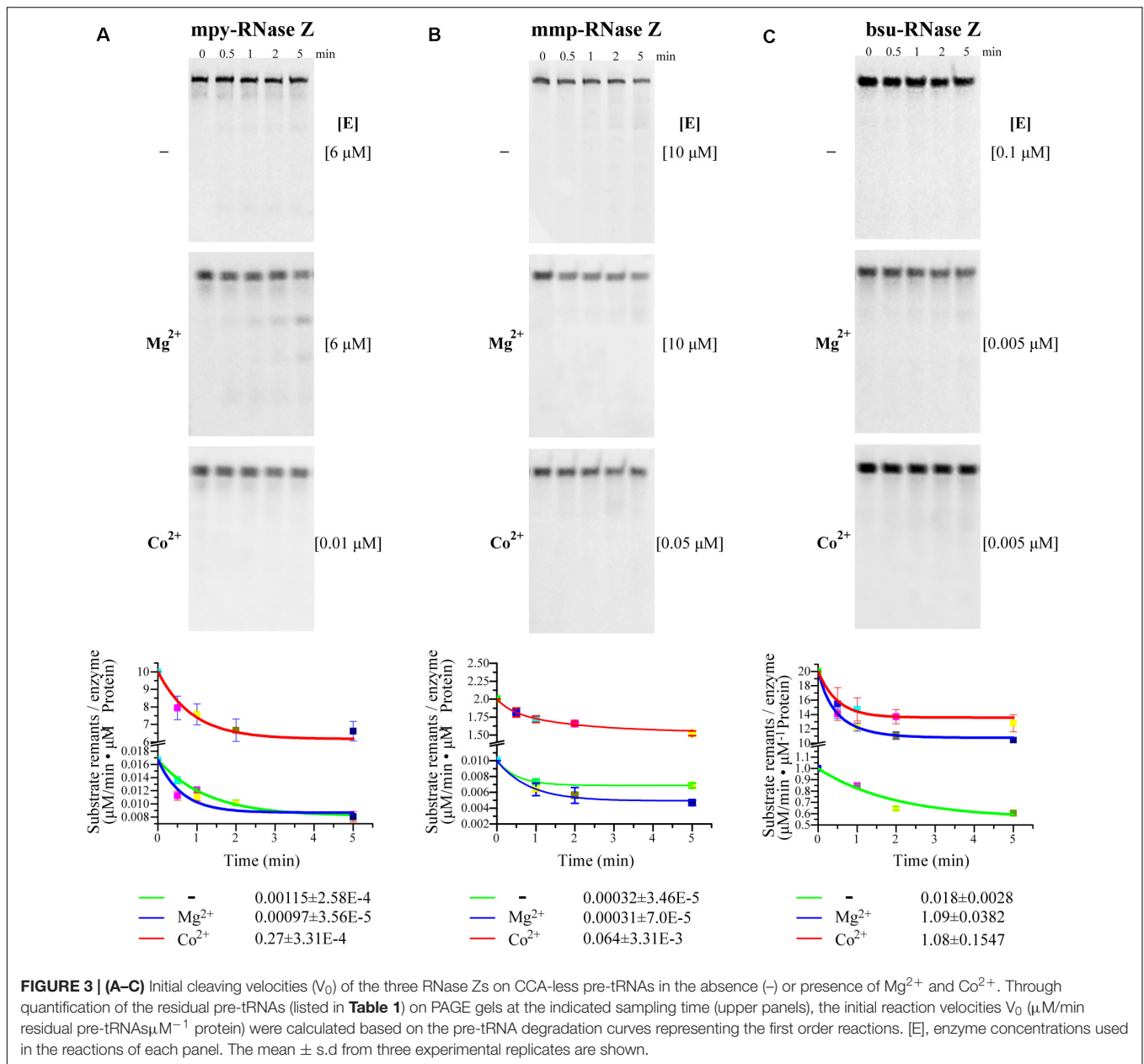
To quantify the effects of Co²⁺ and Mg²⁺, the initial cleavage velocities (V_0) of the three RNase Zs were determined using CCA-less pre-tRNAs as substrates. Through quantifying the substrate residuals within the linear phase during the initial 5 min, it determined that the V_0 ($\mu\text{M}/\text{min}^{-1}$ pre-tRNA $\cdot \mu\text{M}^{-1}$ protein) of mpy-RNase Z and mmp-RNase Z were increased for 235- and 200-fold, respectively, by Co²⁺ supplementation but were not obviously increased by Mg²⁺ supplementation (Figures 3A,B). Whereas, the V_0 of bsu-RNase Z was equally enhanced by Co²⁺ and Mg²⁺ with ~60-fold increase than that of no ion supplementation (Figure 3C).

Further, through replicative quantifying the cleaving velocities on a range of (0.025–1 μM) of the CCA-less pre-tRNA concentrations, kinetic parameters K_m and k_{cat} were further compared for the three RNase Zs in reactions with or without Co²⁺ (Table 1 and Supplementary Figure S4). Supplementation of Co²⁺ slightly (0.43-, 0.47-, and one-fold) affected the K_m values but dramatically elevated the k_{cat} values of mpy-RNase Z, mmp-RNase Z, and bsu-RNase Z for 607-, 1400-, and 34.4-fold,

respectively, and accordingly significantly elevated the cleavage efficiencies (k_{cat}/K_m) of the three RNase Zs for 1400-, 2990-, and 34-fold, respectively (Table 1 and Supplementary Figure S4). Noteworthy, bsu-RNase Z exhibited higher cleavage efficiency than the two aRNase Zs. The k_{cat}/K_m value of bsu-RNase Z is 158- and 644-fold higher than that of mpy- and mmp-RNase Z, respectively, in no metal-ion reactions (Table 1), and the cleavage velocities of the three RNase Zs were evaluated ordered as bsu-RNase Z, mpy-RNase Z, mmp-RNase Z (high to low) (Figure 3). Collectively, Co²⁺ markedly stimulates the activities of the three RNase Zs, and Mg²⁺ also enhances the activity of bsu-RNase Z.

The aRNase Zs Indiscriminately Process Pre-tRNAs With or Without a CCA Motif

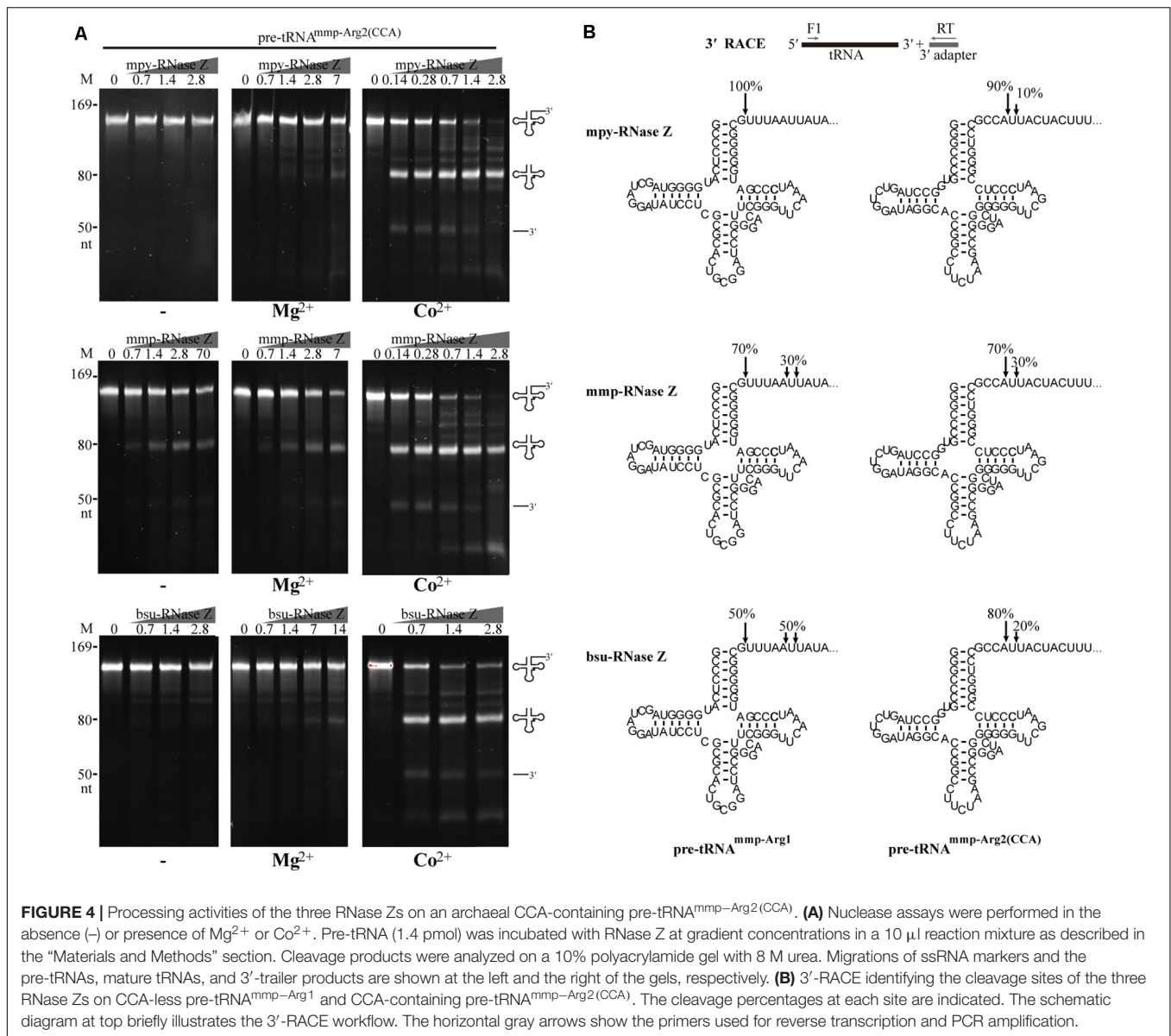
Distinct from the eukaryotic tRNA genes, varying proportions of the prokaryotic tRNA genes genetically encode a CCA motif. For example, 13 of the 52 tRNA genes (25%) in *M. psychrophilus* R15 and 10 of the 38 (26%) in *M. maripaludis* S2 encode the CCA



motif downstream the discriminator nucleotide, respectively (**Supplementary Datasets S2, S3**). To evaluate the activity of aRNase Zs in processing pre-tRNAs with the encoded CCA motif, a CCA-containing pre-tRNA^{mmp-Arg2(CCA)} was used as substrate and bsu-RNase Z was included in parallel (**Figure 4A**). Similar to the activity on CCA-less pre-tRNAs (**Figure 2**), the three RNase Zs all exhibited Co^{2+} and Mg^{2+} stimulated activities on CCA-containing pre-tRNA^{mmp-Arg2(CCA)}; namely, when Co^{2+} supplemented, they efficiently cleaved the CCA-containing pre-tRNA at equivalent low protein to RNA ratios of 1:1 and 5:1 as that on CCA-less ones (**Figure 4A**). Interestingly, mmp-RNase Z even exhibited a higher cleavage activity on CCA-containing pre-tRNAs in the reactions without metal-ion or with Mg^{2+} (**Figures 2, 4A**). While the CCA motif appeared

to suppress the bsu-RNase Z's activity in Mg^{2+} supplemented reaction, as less cleavage products were generated from the CCA-containing pre-tRNA^{mmp-Arg2(CCA)} than from the CCA-less pre-tRNAs (**Figures 2, 4A**).

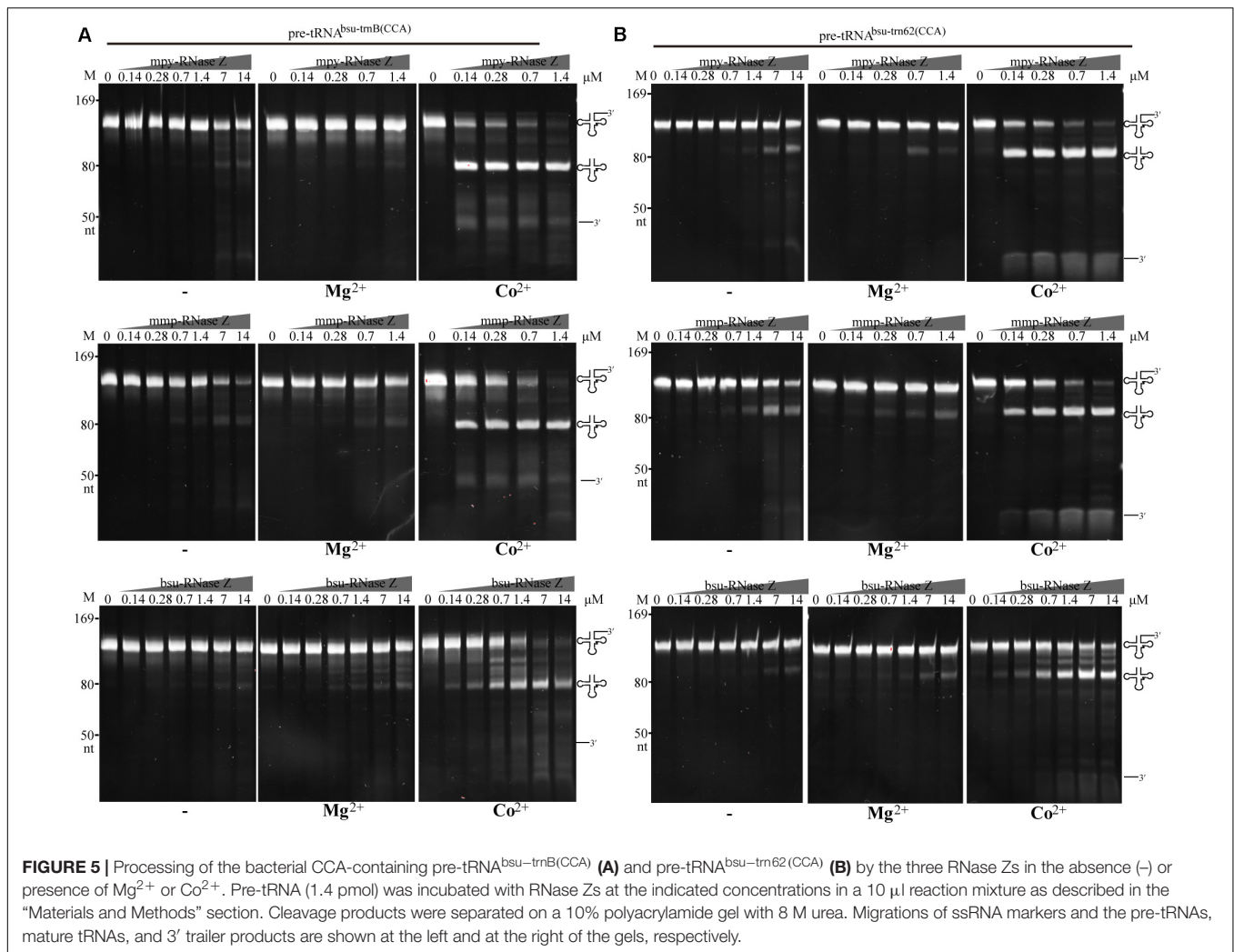
Next, 3'-RACE was performed to determine the cleavage sites in CCA-containing pre-tRNA^{mmp-Arg2(CCA)} and CCA-less pre-tRNA^{mmp-Arg1} of the three RNase Zs in the presence of Co^{2+} (**Figure 4B**). The primary cleaved mature tRNA products were recovered for 3'-end sequencing, which showed that the CCA-less pre-tRNA^{mmp-Arg1} was cleaved primarily downstream the discriminator nucleotide, representing 100%, 70%, and 50% of the cleaving sites generated by mpy-RNase Z, mmp-RNase Z, and bsu-RNase Z, respectively. The remaining 30% and 50% cleaving sites of mmp-RNase Z and bsu-RNase Z were located



five or six nucleotides downstream the discriminator nucleotide, respectively (Figure 4B). Unexpectedly, the CCA-containing pre-tRNA^{mmp-Arg2(CCA)} was mainly cleaved immediate downstream the CCA motif, representing 90%, 70%, and 80% cleaving sites, respectively. The remaining cleavage sites (10%, 30%, and 20%) all located just one nucleotide downstream the CCA motif. Consequently, cleavages of the three RNase Zs on CCA-less pre-tRNAs result in mature tRNA that carries the 3'-end discriminator nucleotide, while cleavages on CCA-containing pre-tRNAs generate mature tRNA ended with the CCA triplet.

Further, three more CCA-containing pre-tRNAs, the *B. subtilis* pre-tRNA^{bsu-trnB(CCA)} and pre-tRNA^{bsu-t62(CCA)} (Figure 5), and the *M. psychrophilus* pre-tRNA^{mpy-Arg2(CCA)} (Supplementary Figure S5), were used as substrates to evaluate the cleavage specificity of the three prokaryotic RNase Zs. Similar to the results with pre-tRNA^{mmp-Arg2(CCA)}

(Figure 4A), the two aRNase Zs at a protein to RNA ratio of 1:1 produced significant amounts of mature tRNAs from the three CCA-containing pre-tRNAs when Co²⁺ supplemented (Figures 5A,B and Supplementary Figure S5), further confirming that they process CCA-containing pre-tRNAs with a comparable activity as CCA-less ones (compare with Figure 2). The two aRNase Zs even exhibited higher activity on CCA-containing than on CCA-less pre-tRNAs in the absence of metal-ion or with Mg²⁺-supplementation (compare Figures 2, 5, and Supplementary Figure S5). However, bsu-RNase Z produced less cleaved products from CCA-containing pre-tRNAs than the two aRNase Zs (Figure 5 and Supplementary Figure S5), indicating a suppression of the CCA motif on the activity of bRNase Z. The CCA motif inhibition on bsu-RNase Z was even more significant in Mg²⁺-supplemented condition, as a



50–100-fold higher protein concentration was required to produce comparable amounts of cleaved product from CCA-containing as CCA-less pre-tRNAs (comparing **Figures 2, 5** and **Supplementary Figure S5**).

The kinetic parameters, K_m and k_{cat} , of the three RNase Zs were then assayed to quantify the cleavage efficiencies on CCA-less vs. CCA-containing pre-tRNAs (**Table 1**). In Co²⁺-amended reactions, K_m values of mpy-RNase Z, mmp-RNase Z, and bsu-RNase Z were 1.65-, 0.69-, and 0.63-fold changed, respectively, on CCA-containing vs. CCA-less pre-tRNAs, suggesting that the pre-tRNA binding affinities of them were slightly affected by the CCA-motif. While, the k_{cat} values of mpy-RNase Z and mmp-RNase Z on CCA-containing pre-tRNAs were 1.38- and 2.14-fold, and the k_{cat}/K_m were 0.83- and 3-fold than those on CCA-less pre-tRNAs, respectively. In contrast, the k_{cat} and k_{cat}/K_m values of bsu-RNase Z on CCA-containing pre-tRNA were 18.7-fold and 11.9-fold lower than those on CCA-less one, respectively. These results indicated that in the presence of Co²⁺, the two aRNase Zs retain nearly indiscriminate cleavage efficiencies on CCA-containing and CCA-less pre-tRNAs, while the catalysis efficiency of the bacterial bsu-RNase Z is inhibited by the CCA-motif.

Consistently, the initial cleavage velocities of the three RNase Zs also supported these conclusions (**Supplementary Figure S6A**).

Based on that 100-fold higher bsu-RNase Z protein was required to process the CCA-containing than the CCA-less pre-tRNA in Mg²⁺-amended reaction, the CCA-motif was reported to inhibit the activity of bsu-RNase Z (Pellegrini et al., 2003). In this study, the initial velocity of bsu-RNase Z on CCA-containing pre-tRNA was determined to be 1520-fold lower than that on CCA-less one in Mg²⁺-amended reaction (**Supplementary Figure S6B**), while be only 5.8-fold lower in Co²⁺ supplementation (**Supplementary Figure S6A**). Therefore, these indicated that although the encoded CCA motif severely inhibits the activity of bsu-RNase Z, Co²⁺-supplementation could dramatically ameliorate the inhibition.

The aRNase Zs Require 5' Matured Pre-tRNA for 3'-End Processing

Most of RNase Zs analyzed so far appear requiring a mature tRNA 5'-end for 3'-end processing (Kunzmann et al., 1998; Nashimoto et al., 1999b; Schierling et al., 2002; Pellegrini et al., 2003), so the

5'-leader removal is assumed preceding the 3'-end processing of pre-tRNAs by RNase Z (Redko et al., 2007). To evaluate the effect of the pre-tRNA 5' extensions on the 3'-end processing of aRNase Zs, pre-tRNA^{mpy-Arg1} and pre-tRNA^{mmp-Arg1} that carry varying lengths of 5' extensions were used as substrates. The cleavage assays showed that although the two aRNase Zs processed the 5' extended pre-tRNAs, lower 3'-trailer processing activities were observed for those with longer 5' extensions. In detail, ≥ 10 nt 5' extensions markedly suppressed the 3'-end processing activity of mpy-RNase Z (Figure 6A), while a 5 nt-5' extension already inhibited mmp-RNase Z (Figure 6B).

Effect of the 3'-trailer lengths on the activities of two aRNase Zs were also assayed. The results showed that mpy-RNase Z and mmp-RNase Z could efficiently cleave all tested pre-tRNAs with various lengths of 3'-trailer, although reduced activity was found on a 150 nt-3'-trailer (Figures 6C,D). These results demonstrate that the two aRNase Zs only efficiently process the 3'-ends of pre-tRNAs that have matured 5'-ends, but regardless, the 3'-trailer lengths, that is, RNase P cleavage to produce a mature 5'-end should precede the 3'-trailer processing by RNase Z.

The aRNase Zs but Not the bRNase Z Process Intron-Containing Pre-tRNAs

Considering that some archaeal pre-tRNAs contain introns (Tocchini-Valentini et al., 2005), we then evaluated the processing activities of the two aRNase Zs on pre-tRNA^{mpy-Arg3(intron)} and pre-tRNA^{mpy-Tyr(intron)} that contain 24 nt- and 38 nt-long introns, respectively. Cleavage assays determined that the two aRNase Zs were capable of cleaving the intron-containing pre-tRNAs but with lower efficiency than on intron-less pre-tRNAs. In contrast, no detectable activity was found for bsu-RNase Z on processing the intron-containing pre-tRNAs (Figure 7). The capability of the aRNase Zs, but not the bRNase Z, in processing the intron-containing pre-tRNAs complies with the fact that the intron-carrying pre-tRNAs are present in archaea but not in bacteria (Tocchini-Valentini et al., 2005).

Two aRNase Zs Process Aberrant Pre-tRNAs, but the Acceptor Stem Is Indispensable

Next, we assayed the requirements of tRNA elements by aRNase Zs in processing the pre-tRNA 3'-end. An array of tRNA variants that lack the D arm, anticodon arm, T arm, or acceptor stem but carry a 30 nt-3'-trailer were used as substrates (Figure 8). Each of the aberrant pre-tRNAs was incubated with the two aRNase Zs. In the presence of Co²⁺, the two aRNase Zs processed all the pre-tRNA variants at a comparable efficiency as the wild-type pre-tRNA, except for the variant that lacks the acceptor stem. However, in Mg²⁺-supplemented reactions, lacking any element resulted in a markedly reduced processing efficiency of mmp-RNase Z; while deletion of the T arm or acceptor stem, but not the D and anticodon arms, suppressed the activity of mpy-RNase Z. This indicates that as long as Co²⁺ is present, the aRNase Zs are capable of processing pre-tRNAs without the D, the anticodon, or the T arm, but the acceptor stem is indispensable, implying that

the aRNase Zs could have a broad *in vivo* substrate spectrum in addition to pre-tRNAs.

DISCUSSION

Thus far, our knowledge about the properties of methanomicrobial aRNase Zs, particularly in processing the CCA-containing pre-tRNAs, remains limited. The present study has comprehensively examined the biochemical characteristics of two aRNase Zs from methanomicrobial archaea. We found that Co²⁺ markedly activates the pre-tRNA 3'-end processing efficiencies of the two aRNase Zs for 1440- and 2990-fold, respectively, and even is indispensable to the aRNase Zs. Distinctively, the two aRNase Zs indiscriminately process CCA-containing and CCA-less pre-tRNAs with similar catalytic efficiency (k_{cat}/K_m) and generate the mature tRNA ended with CCA in the former and the discriminator nucleotide in the latter, respectively. Moreover, Co²⁺ not only activates the pre-tRNA processing activity of the bRNase Z but also ameliorates the CCA motif inhibitory effect from 1520-fold to 5.8-fold. Noticeably, the two methanomicrobial aRNase Zs are capable of processing intron-containing pre-tRNAs and aberrant pre-tRNA mutants that lack the T, D, or anticodon arm, but require the acceptor stem and mature 5'-end for 3'-end processing. Collectively, this work elucidates the characteristics of methanomicrobial aRNase Zs, in particular the capability of processing CCA-containing pre-tRNAs, which could be shared by aRNase Z orthologs that are ubiquitously distributed in archaea.

Co²⁺, Mn²⁺, and Mg²⁺ Appear to Be Required by Most Prokaryotic RNase Zs

Though RNase Z affiliates with the β -lactamase family metalloproteins and Zn²⁺ (one or two) coordinated in the metallo- β -lactamase domain has been observed in the RNase Zs from *B. subtilis* (Li de la Sierra-Gallay et al., 2005), *T. maritima* (Ishii et al., 2005), and *E. coli* (Kostelecny et al., 2006), Zn²⁺ addition neither promotes the activities of the archaeal nor the bRNase Zs (Supplementary Figure S3). On the contrary, this work found that Co²⁺ supplementation markedly enhances the 3'-end processing activities of both the archaeal and bRNase Zs, regardless of the pre-tRNAs from archaeal or bacteria or containing the CCA motif or not (Table 1 and Figures 2, 3, 4A, 5 and Supplementary Figures S3–S6). In addition to Co²⁺, Mg²⁺ also promotes the activity of the bacterial bsu-RNase Z (Figures 2, 3, 5). Co²⁺ stimulation on *E. coli* RNase Z was reported in an earlier study (Asha et al., 1983), and Mn²⁺ has similar effect in stimulating the activities of RNase Zs from *T. maritima* (Minagawa et al., 2006), *A. thaliana* (Spath et al., 2007), *H. volcanii*, and *P. furiosus* (Spaeth et al., 2008). Therefore, the stimulatory effects of Co²⁺, Mn²⁺, and Mg²⁺ could be the common property among RNase Zs from eukaryotes, archaea, and bacteria. These metal ions might help pre-tRNA fold properly, or induce RNase Z to attain an active conformation and/or assist RNase Z to interact with pre-tRNA correctly. However, to unveil the underlying mechanisms, further studies are required, such as to solve the structures of the apo or

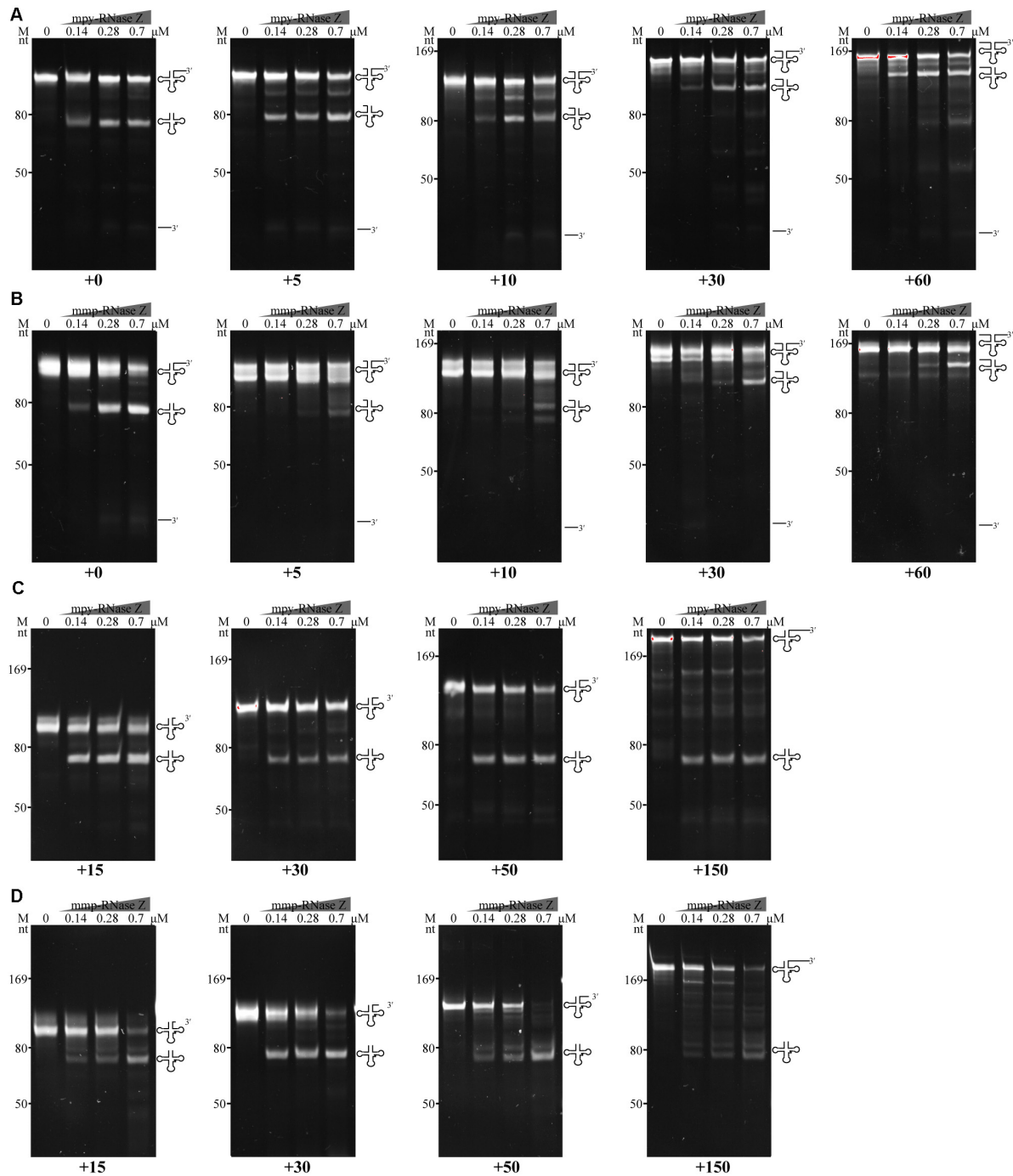


FIGURE 6 | Effects of 5' and 3' extensions on the 3'-end processing of pre-tRNAs by (A,C) mpy-RNase Z and (B,D) mmp-RNase Z. (A,B) Pre-tRNA^{mpy-Arg1} and pre-tRNA^{mmp-Arg1} carrying a 30 nt 3'-trailer and 5' extensions with 0, 5, 10, 30, or 60 nt were used as substrates. (C,D) Pre-tRNA^{mpy-Arg1} and pre-tRNA^{mmp-Arg1} with no 5' extension but carrying 3'-trailers of 15, 30, 50, or 150 nt were used as substrates. Pre-tRNA (1.4 pmol) was incubated with purified RNase Zs at gradient concentrations in a 10 μ l reaction mixture as described in the "Materials and Methods" section. The cleavage products were separated on a 10% polyacrylamide gel with 8 M urea. Migration of ssRNA markers, the pre-tRNAs, mature tRNAs, and 3'-trailer products are indicated at the left and at the right of the gels, respectively.

pre-tRNA-complexed RNase Z with or without a metal ligand to compare the detailed conformation changes.

Although bsu-RNase Z and the two aRNase Zs have similar key elements and conserved sequences as indicated by the

protein sequence alignment (**Supplementary Figure S1**), higher cleavage velocity and efficiency have been found for bsu-RNase Z even without the addition of metal ions (**Figure 3** and **Table 1**). This could be attributed to a higher metal

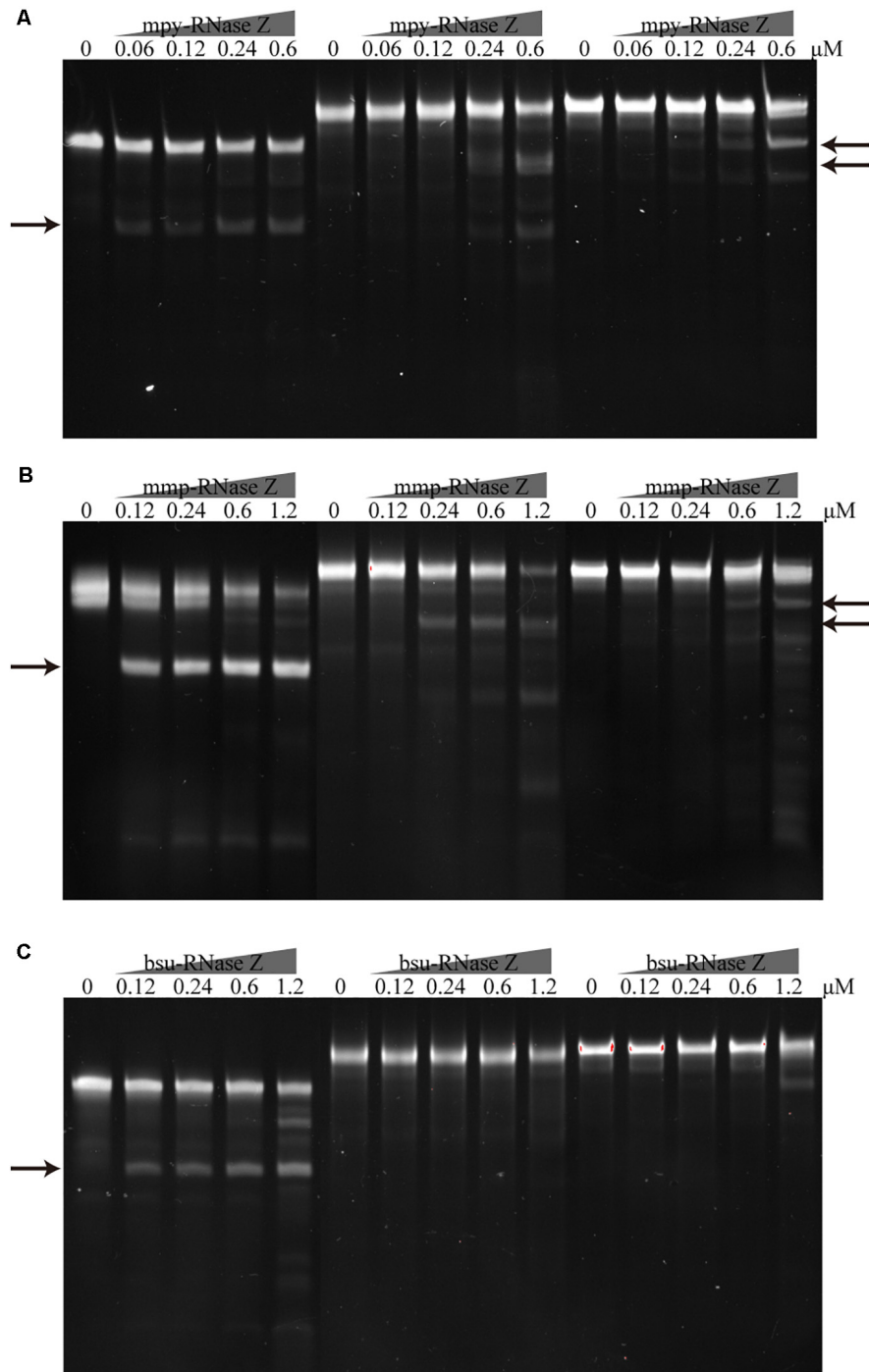
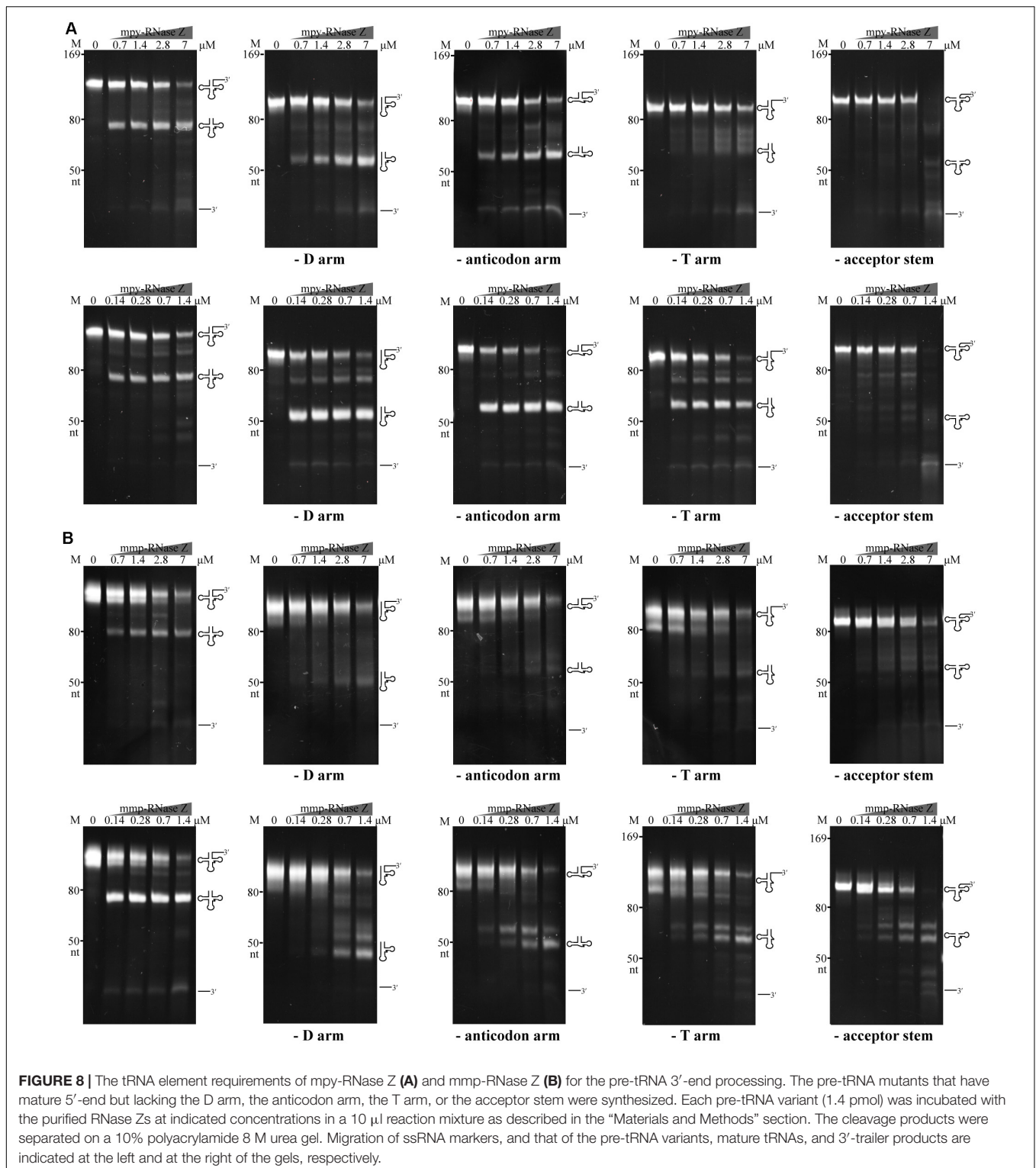


FIGURE 7 | Processing of the intron containing pre-tRNAs by the archaeal and bacterial RNase Zs. The intron-less pre-tRNA^{mpy}-Arg¹ and the intron-containing pre-tRNA^{mpy}-Arg³(intron) and pre-tRNA^{mpy}-Tyr(intron) were each incubated with **(A)** *mpy*-RNase Z, **(B)** *mmp*-RNase Z, and **(C)** *bsu*-RNase Z. Pre-tRNA^{mpy}-Arg³(intron) and pre-tRNA^{mpy}-Tyr(intron) contain 24 and 38 nt introns, respectively. Pre-tRNA (1.2 pmol) was incubated with purified RNase Z at the indicated concentrations in a 10 μl reaction mixture as described in the “Materials and Methods” section. The cleavage products were separated on a 10% polyacrylamide 8 M urea gel and are indicated by arrows.

affinity of *bsu*-RNase Z, in which more metal ions have been already sequestered during purification. Supportively, a higher EDTA concentration was needed to inhibit the cleavage

activity of *bsu*-RNase Z than that to the two *a*RNase Zs (**Supplementary Figure S7**). Moreover, the *a*RNase Zs rely more on Co²⁺ than *bsu*-RNase Z (**Supplementary Figure S3** and



Figures 2, 3 and Table 1), while the latter is also activated by Mg^{2+} (Figures 2, 3 and Table 1), implying that the aRNase Zs have a better adaptation to Co^{2+} and bsu-RNase Z to Mg^{2+} . It is assumed that bacteria have higher cellular levels of Mg^{2+} and Mn^{2+} , but the methanomicrobial archaea

contain higher Co^{2+} . Cobalt is used as a metal ligand in some methanomicrobial enzymes, for example, the methanol and methyl amine methyltransferases are all corrinoid proteins, and Co^{2+} is routinely supplemented in the culture media of methanogens (Sarmiento et al., 2011). This could be a

circumstantial evidence that aRNase Zs rely more on Co^{2+} , while the bRNase Zs are better adapted to Mg^{2+} .

Co²⁺ Is Specifically Required for RNase Zs in Processing CCA-Containing Pre-tRNAs

This work found that the aRNase Zs exhibit a comparable activity of processing the CCA-containing and CCA-less pre-tRNAs (Figures 2–5 and Supplementary Figures S4–S6) and retain similar k_{cat}/K_m values (Table 1) and generate matured tRNA 3'-ends with CCA in the former and the discriminator nucleotide in the latter. Therefore, aRNase Z could be the single ribonuclease functioning in the maturation of tRNA 3'-ends in archaea; this is different from that in bacteria, in which not only RNase Z-dependent endonucleolytic maturation but also additional exonucleolytic pathway through collaboration of several enzymes both exist (Redko et al., 2007). The CCA-containing pre-tRNA genes, with varying proportions, are distributed in many archaeal genomes; for example, 26% and 25% of tRNA genes in *M. maripaludis* S2 and *M. psychrophilus* R15 contain the CCA motif (Supplementary Datasets S2, S3), respectively. Thus, we hypothesized that RNase Z-mediated single-step endoribonucleolytic cleavage plays a primary role in archaeal tRNA 3'-end maturation, as that in eukaryotes (Castano et al., 1985; Friendewey et al., 1985; Stange and Beier, 1987; Oommen et al., 1992). Although this hypothesis is not yet verified *in vivo*, the gene-encoding mmp-RNase Z has been determined as essential in *M. maripaludis* (Sarmiento et al., 2013), providing a circumstantial evidence for the key functions of aRNase Z, presumably through the single-step tRNA 3'-end maturation.

Consistent with the previous findings (Pellegrini et al., 2003), the present work found that the CCA motif exerts an obvious inhibitory effect on the bacterial *bsu*-RNase Z. However, this inhibitory effect was significantly reduced when Co^{2+} was amended (Figures 3–5 and Supplementary Figures S5, S6 and Table 1). Similarly, the *E. coli* RNase Z was reported to process the CCA-containing pre-tRNAs in the presence of Co^{2+} (Dutta et al., 2012), and actually involved in the maturation of all 86 CCA-containing pre-tRNAs when RNases T, PH, D, and II are absent (Kelly and Deutscher, 1992), so it can be one primary player in tRNA 3'-end maturation as well. The *T. maritima* RNase Z also exhibited a cleavage activity downstream the CCA motifs of 45 CCA-containing tRNAs (Minagawa et al., 2004). Thus, both bacterial and aRNase Zs are capable of processing CCA-containing pre-tRNAs and expose the genetically encoded CCA triplet. This also suggests that RNase Z-mediated one-step processing on the CCA-containing pre-tRNAs could be a widely distributed mode in prokaryotes.

Substrate Recognition and Processing Order of the Methanomicrobial aRNase Zs in Pre-tRNA Maturation

The present work found that ≥ 10 nt 5' extensions markedly suppressed the pre-tRNAs processing efficiency of the aRNase

Zs, suggesting that a mature 5'-end is a precondition for 3' maturation of pre-tRNAs (Figures 6A,B). Similar observations were found in *B. subtilis* RNase Z, which exhibited a reduced 3'-end processing activity on pre-tRNAs having ≥ 33 nt 5' extensions (Pellegrini et al., 2003); while the pig liver RNase Z even lost its 3'-end processing activity on pre-tRNAs with 5' extensions > 9 nt (Nashimoto et al., 1999a). Thus, analogous to the eukaryotic and bacterial pre-tRNA processing procedures, RNase P-mediated 5'-end processing could precede the 3'-end processing by RNase Z in methanomicrobial archaea.

While, the 3' extension lengths did not exhibit inhibitory effects on the two aRNase Zs, which showed nearly indiscriminate processing activities on pre-tRNAs with diverse 3' extensions (Figures 6C,D). Moreover, the two aRNase Zs are capable of processing intron-containing pre-tRNAs though with a lower efficiency (Figure 7), so they could be involved in maturation of the inherited intron-containing pre-tRNAs in archaea (Tocchini-Valentini et al., 2005; Supplementary Dataset S2). This also suggests that aRNase Zs could process the 3'-end before the intron removal when the tRNA precursors are at high concentrations, while intron scissoring may occur first when the precursors are at physiological concentrations.

In addition, the two methanomicrobial aRNase Zs indiscriminately process the homologous and heterologous tRNA precursors, indicating that they recognize tRNA structures but not the sequences. Enzymatic assays on the pre-tRNA element mutants determined that the acceptor stem, but not the D, anticodon, and T arms, is required for aRNase Zs in the tRNA 3'-end maturation in the presence of Co^{2+} (Figure 8). In support of these observations, a tRNA-bound structure of the *B. subtilis* RNase Z has revealed the direct interactions of the T-arm and the acceptor stem with the flexible arm and helix $\alpha 7$ of the RNase Z dimer, while the D-arm and anticodon loop are dispensable in the interaction, and the tRNA phosphodiester backbone is primarily recognized (Li de la Sierra-Gallay et al., 2006). Therefore, these interactions enable RNase Zs adapted to a wide variety of tRNA substrates.

In conclusion, in the presence of Co^{2+} , the methanomicrobial aRNase Zs are capable of processing the 3'-end of various pre-tRNA species, including CCA-containing and CCA-less, intron-containing, and T-, D-, and anticodon-arm-lacking tRNA precursors, hinting their pivotal roles in pre-tRNA 3'-end maturation and a potential broad substrate spectrum, so aRNase Zs could fulfill a plethora of functions in RNA metabolism in archaea.

DATA AVAILABILITY STATEMENT

All datasets generated for this study are included in the article/Supplementary Material.

AUTHOR CONTRIBUTIONS

JL and XD conceptualized the experiments and acquired funding. XW, XG, and JL designed and performed the biochemical

experiments. LY performed the protein expression and 3'-RACE experiments. All of the researchers interpreted the experimental data and assisted with the preparation of the manuscript. JL, DL, and XD wrote the manuscript. All authors approved the final manuscript.

FUNDING

This work was supported by the National Natural Science Foundation of China under grant nos. 91751203 and 31670049, the National Key R&D Program of China under grant nos. 2020YFA0906800, 2019YFA0905500, and 2018YFC0310800.

ACKNOWLEDGMENTS

The authors thank LetPub (www.letpub.com) for linguistic assistance on the manuscript preparation.

SUPPLEMENTARY MATERIAL

The Supplementary Material for this article can be found online at: <https://www.frontiersin.org/articles/10.3389/fmicb.2020.01851/full#supplementary-material>

FIGURE S1 | Sequence alignment of the RNase Z family proteins. The protein sequences were aligned using ClustalW program (Larkin et al., 2007) and the diagram was prepared using ESPript program (Gouet et al., 1999). Identical residues are highlighted with white type on a red background and similar residues are shown as red type. *Methanobolbus psychrophilus* RNase Z (Mpsy_2804) and *Methanococcus maripaludis* (MMP0906) shares 38% and 58% amino-acid sequence identity and similarity, respectively. Secondary structural elements of bsu-RNase Z (PDB ID: 1Y44) are shown on the top of the sequence. *Bacillus subtilis* RNase Z (bsu: Bsu23480) shares 48%, 42%, 42%, 36%, 36%, 32%, 33%, 33%, and 28% amino acid sequence identity to *Escherichia coli* RNase Z (eco: b2268), *M. maripaludis* RNase Z (mmp: MMP0906), *Methanocaldococcus jannaschii* RNase Z (mja: MJ_1502), *M. psychrophilus* RNase Z (mpy: Mpsy_2804), *Haloferax volcanii* RNase Z (hvo: HVO_0144), *Pyrococcus furiosus* RNase Z (pfu: PF12345), *Thermoplasma acidophilum* RNase Z (tac: Tal155), *Pyrobaculum aerophilum* RNase Z (pai: PF12345), and *Thermotoga maritima* RNase Z (tma: TM0864), respectively.

REFERENCES

- Asha, P. K., Blouin, R. T., Zaniewski, R., and Deutscher, M. P. (1983). Ribonuclease BN: identification and partial characterization of a new tRNA processing enzyme. *Proc. Natl. Acad. Sci. U.S.A.* 80, 3301–3304. doi: 10.1073/pnas.80.11.3301
- Callebaut, I., Moshous, D., Mornon, J. P., and De Villartay, J. P. (2002). Metallo-beta-lactamase fold within nucleic acids processing enzymes: the beta-CASP family. *Nucleic Acids Res.* 30, 3592–3601. doi: 10.1093/nar/gkf470
- Castano, J. G., Tobian, J. A., and Zasloff, M. (1985). Purification and characterization of an endonuclease from *Xenopus laevis* ovaries which accurately processes the 3' terminus of human pre-tRNA-Met(i) (3' pre-tRNAse). *J. Biol. Chem.* 260, 9002–9008.
- Ceballos-Chavez, M., and Vioque, A. (2005). Sequence-dependent cleavage site selection by RNase Z from the cyanobacterium *Synechocystis* sp.

FIGURE S2 | SDS-PAGE of the three RNase Zs tested in this study. The purified His₆-tagged recombinant RNase Z proteins on 12% SDS-PAGE were shown. M, the protein ladders indicated at the left to identify the migration positions of the proteins.

FIGURE S3 | Stimulatory effects of Co²⁺ or Mg²⁺ on the tRNA 3'-end processing activity of the archaeal and bacterial RNase Zs. Two pre-tRNAs were used as substrates, that is, (A) *M. maripaludis* S2 pre-tRNA^{mmp-Arg1} and (B) *B. subtilis* pre-tRNA^{bsu-trnl}. Purified mpy-RNase Z from *M. psychrophilus*, mmp-RNase Z from *M. maripaludis*, and bsu-RNase Z from *B. subtilis* were assayed in the absence (–) or presence (+) of 1 mM Zn²⁺, Cu²⁺, Co²⁺, or Mg²⁺. Pre-tRNA (1.4 pmol) was incubated with 0.7 μM mpy-RNase Z, 0.7 μM mmp-RNase Z, and 0.28 μM bsu-RNase Z at 37°C for 30 min. The cleavage products were separated on a 10% polyacrylamide 8 M urea gel. Migration of the ssRNA markers with indicated lengths and migration of the pre-tRNAs, mature tRNAs, and 3'-trailer products are marked at the left and at the right of gels, respectively.

FIGURE S4 | The Lineweaver–Burk plots of the kinetic parameters of the three RNase Zs for processing the CCA-containing (CCA+) and CCA-less (CCA–) pre-tRNAs in the absence (–) or presence (+) of Co²⁺. A range of (0.025–1 μM) pre-tRNA (Table 1) substrate concentrations were assayed for each tested RNase Z at 37°C. The initial velocity (V₀) of RNase Z at each substrate concentration was determined through quantifying the substrate residuals in the linear phase during the initial 5 min similarly as that shown in Figure 3. The kinetic parameters of K_m, V_{max}, and K_{cat} were obtained by fitting the Lineweaver–Burk plotting data to the Michaelis-Menten equation.

FIGURE S5 | Ribonuclease assays of the processing activity of the three RNase Zs on the CCA containing *M. psychrophilus* pre-tRNA^{mpy-Arg2(CCA)} in the absence (–) or presence of Mg²⁺ or Co²⁺. Pre-tRNA (1.4 pmol) was incubated with purified recombinant RNase Z at gradient concentrations in a 10 μl nuclease reaction as described in the “Materials and Methods” section. Cleavage products were separated on a 10% polyacrylamide 8 M urea gel. The migration of ssRNA markers and the migration of pre-tRNAs, mature tRNAs, and 3'-trailer products are labeled at the left and at the right of the gels, respectively.

FIGURE S6 | Comparison of the initial velocities of the three RNase Zs for processing the CCA-less and CCA-containing pre-tRNAs in Co²⁺ supplementation (A) and in Mg²⁺ supplementation for bsu-RNase Z (B). Initial reaction velocities (V₀) were determined by quantifying the residual pre-tRNA substrate amounts (listed in Table 1) on PAGE gels at each sampling time, which are shown as attenuation curves of pre-tRNA remnants per the enzyme amounts in the upper panels. Values of V₀ (μM/min residual pre-tRNAs·μM⁻¹ protein) indicated below the panels are the mean ± s.d from three experimental replicates.

FIGURE S7 | EDTA inhibition on the 3'-processing activity of the three RNase Zs. EDTA concentrations were shown on the top of the gel. CK, control reactions without enzyme.

TABLE S1 | Primers used in this study.

TABLE S2 | Sequences of RNA substrates used in this study.

- PCC 6803. *J. Biol. Chem.* 280, 33461–33469. doi: 10.1074/jbc.m504691200
- Cudny, H., and Deutscher, M. P. (1986). High-level overexpression, rapid purification, and properties of *Escherichia coli* tRNA nucleotidyltransferase. *J. Biol. Chem.* 261, 6450–6453.
- Cudny, H., Lupski, J. R., Godson, G. N., and Deutscher, M. P. (1986). Cloning, sequencing, and species relatedness of the *Escherichia-Coli* cca gene encoding the enzyme transfer-RNA nucleotidyltransferase. *J. Biol. Chem.* 261, 6444–6449.
- Dutta, T., and Deutscher, M. P. (2009). Catalytic properties of RNase BN/RNase Z from *Escherichia coli* RNase BN is both an exo- and endoribonuclease. *J. Biol. Chem.* 284, 15425–15431. doi: 10.1074/jbc.m109.005462
- Dutta, T., Malhotra, A., and Deutscher, M. P. (2012). Exoribonuclease and endoribonuclease activities of RNase BN/RNase Z both function in Vivo. *J. Biol. Chem.* 287, 35747–35755. doi: 10.1074/jbc.m112.407403

- Eme, L., Spang, A., Lombard, J., Stairs, C. W., and Ettema, T. J. G. (2017). Archaea and the origin of eukaryotes. *Nat. Rev. Microbiol.* 15, 711–723. doi: 10.1038/nrmicro.2017.133
- Evans, P. N., Boyd, J. A., Leu, A. O., Woodcroft, B. J., Parks, D. H., Hugenholtz, P., et al. (2019). An evolving view of methane metabolism in the Archaea. *Nat. Rev. Microbiol.* 17, 219–232. doi: 10.1038/s41579-018-0136-7
- Ezraty, B., Dahlgren, B., and Deutscher, M. P. (2005). The RNase Z homologue encoded by *Escherichia coli* elcA gene is RNase BN. *J. Biol. Chem.* 280, 16542–16545. doi: 10.1074/jbc.c500098200
- Frendewey, D., Dinger, T., Cooley, L., and Soll, D. (1985). Processing of precursor tRNAs in *Drosophila*. Processing of the 3' end involves an endonucleolytic cleavage and occurs after 5' end maturation. *J. Biol. Chem.* 260, 449–454.
- Gouet, P., Courcelle, E., Stuart, D. I., and Metz, F. (1999). ESPript: analysis of multiple sequence alignments in PostScript. *Bioinformatics* 15, 305–308. doi: 10.1093/bioinformatics/15.4.305
- Guerritakada, C., Gardiner, K., Marsh, T., Pace, N., and Altman, S. (1983). The RNA moiety of Ribonuclease-P is the catalytic subunit of the enzyme. *Cell* 35, 849–857. doi: 10.1016/0092-8674(83)90117-4
- Hoang, D. T., Chernomor, O., Von Haeseler, A., Minh, B. Q., and Vinh, L. S. (2018). UFBoot2: improving the ultrafast bootstrap approximation. *Mol. Biol. Evol.* 35, 518–522. doi: 10.1093/molbev/msx281
- Holzmann, J., Frank, P., Löffler, E., Bennett, K. L., Gerner, C., and Rossmann, W. (2008). RNase P without RNA: identification and functional reconstitution of the human mitochondrial tRNA processing enzyme. *Cell* 135, 462–474. doi: 10.1016/j.cell.2008.09.013
- Ishii, R., Minagawa, A., Takaku, H., Takagi, M., Nashimoto, M., and Yokoyama, S. (2008). Crystal structure of the tRNA 3' processing endoribonuclease tRNase Z from *Thermotoga maritima*. *J. Biol. Chem.* 280, 14138–14144.
- Kalyaanamoorthy, S., Minh, B. Q., Wong, T. K. F., Von Haeseler, A., and Jermin, L. S. (2017). ModelFinder: fast model selection for accurate phylogenetic estimates. *Nat. Methods* 14, 587–589. doi: 10.1038/nmeth.4285
- Kelly, K. O., and Deutscher, M. P. (1992). The presence of only one of five exoribonucleases is sufficient to support the growth of *Escherichia coli*. *J. Bacteriol.* 174, 6682–6684. doi: 10.1128/jb.174.20.6682-6684.1992
- Kirchner, S., and Ignatova, Z. (2015). Emerging roles of tRNA in adaptive translation, signalling dynamics and disease. *Nat. Rev. Genet.* 16, 98–112. doi: 10.1038/nrg3861
- Kostecky, B., Pohl, E., Vogel, A., Schilling, O., and Meyer-Klaucke, W. (2006). The crystal structure of the zinc phosphodiesterase from *Escherichia coli* provides insight into function and cooperativity of tRNase Z-family proteins. *J. Bacteriol.* 188, 1607–1614. doi: 10.1128/jb.188.4.1607-1614.2006
- Kunzmann, A., Brennicke, A., and Marchfelder, A. (1998). 5' end maturation and RNA editing have to precede tRNA 3' processing in plant mitochondria. *Proc. Natl. Acad. Sci. U.S.A.* 95, 108–113. doi: 10.1073/pnas.95.1.108
- Larkin, M. A., Blackshields, G., Brown, N. P., Chenna, R., McGettigan, P. A., McWilliam, H., et al. (2007). Clustal W and Clustal X version 2.0. *Bioinformatics* 23, 2947–2948. doi: 10.1093/bioinformatics/btm404
- Letunic, I., and Bork, P. (2016). Interactive tree of life (iTOL) v3: an online tool for the display and annotation of phylogenetic and other trees. *Nucleic Acids Res.* 44, W242–W245.
- Li, Z., and Deutscher, M. P. (1996). Maturation pathways for *E. coli* tRNA precursors: a random multienzyme process in vivo. *Cell* 86, 503–512. doi: 10.1016/s0092-8674(00)80123-3
- Li, Z., and Deutscher, M. P. (2002). RNase E plays an essential role in the maturation of *Escherichia coli* tRNA precursors. *RNA* 8, 97–109. doi: 10.1017/s1355838202014929
- Li de la Sierra-Gallay, I., Mathy, N., Pellegrini, O., and Condon, C. (2006). Structure of the ubiquitous 3' processing enzyme RNase Z bound to transfer RNA. *Nat. Struct. Mol. Biol.* 13, 376–377. doi: 10.1038/nsmb1066
- Li de la Sierra-Gallay, I., Pellegrini, O., and Condon, C. (2005). Structural basis for substrate binding, cleavage and allostery in the tRNA maturase RNase Z. *Nature* 433, 657–661. doi: 10.1038/nature03284
- Minagawa, A., Takaku, H., Ishii, R., Takagi, M., Yokoyama, S., and Nashimoto, M. (2006). Identification by Mn²⁺ rescue of two residues essential for the proton transfer of tRNase Z catalysis. *Nucleic Acids Res.* 34, 3811–3818. doi: 10.1093/nar/gkl517
- Minagawa, A., Takaku, H., Takagi, M., and Nashimoto, M. (2004). A novel endonucleolytic mechanism to generate the CCA 3' termini of tRNA molecules in *Thermotoga maritima*. *J. Biol. Chem.* 279, 15688–15697. doi: 10.1074/jbc.m313951200
- Mohan, A., Whyte, S., Wang, X., Nashimoto, M., and Levinger, L. (1999). The 3' end CCA of mature tRNA is an antideterminant for eukaryotic 3'-tRNase. *RNA* 5, 245–256. doi: 10.1017/s1355838299981256
- Mohanty, B. K., Petree, J. R., and Kushner, S. R. (2016). Endonucleolytic cleavages by RNase E generate the mature 3' termini of the three proline tRNAs in *Escherichia coli*. *Nucleic Acids Res.* 44, 6350–6362. doi: 10.1093/nar/gkw517
- Nashimoto, M. (1997). Distribution of both lengths and 5' terminal nucleotides of mammalian pre-tRNA 3' trailers reflects properties of 3' processing endoribonuclease. *Nucleic Acids Res.* 25, 1148–1154. doi: 10.1093/nar/25.6.1148
- Nashimoto, M., Tamura, M., and Kaspar, R. L. (1999a). Selection of cleavage site by mammalian tRNA 3' processing endoribonuclease. *J. Biol. Chem.* 274, 727–740. doi: 10.1006/jmbi.1999.2639
- Nashimoto, M., Wesemann, D. R., Geary, S., Tamura, M., and Kaspar, R. L. (1999b). Long 5' leaders inhibit removal of a 3' trailer from a precursor tRNA by mammalian tRNA 3' processing endoribonuclease. *Nucleic Acids Res.* 27, 2770–2776. doi: 10.1093/nar/27.13.2770
- Nguyen, L. T., Schmidt, H. A., Von Haeseler, A., and Minh, B. Q. (2015). IQ-TREE: a fast and effective stochastic algorithm for estimating maximum-likelihood phylogenies. *Mol. Biol. Evol.* 32, 268–274. doi: 10.1093/molbev/msu300
- Niedner, A., Müller, M., Moorthy, B. T., Jansen, R. P., and Niessing, D. (2013). Role of Loc1p in assembly and reorganization of nuclear ASH1 messenger ribonucleoprotein particles in yeast. *Proc. Natl. Acad. Sci. U.S.A.* 110, E5049–E5058.
- Oommen, A., Li, X. Q., and Gegenheimer, P. (1992). Cleavage specificity of chloroplast and nuclear tRNA 3'-processing nucleases. *Mol. Cell Biol.* 12, 865–875. doi: 10.1128/mcb.12.2.865
- Ow, M. C., and Kushner, S. R. (2002). Initiation of tRNA maturation by RNase E is essential for cell viability in *E. coli*. *Genes Dev.* 16, 1102–1115. doi: 10.1101/gad.983502
- Pellegrini, O., Nezzar, J., Marchfelder, A., Putzer, H., and Condon, C. (2003). Endonucleolytic processing of CCA-less tRNA precursors by RNase Z in *Bacillus subtilis*. *EMBO J.* 22, 4534–4543. doi: 10.1093/emboj/cdg435
- Qi, L., Yue, L., Feng, D., Qi, F., Li, J., and Dong, X. (2017). Genome-wide mRNA processing in methanogenic archaea reveals post-transcriptional regulation of ribosomal protein synthesis. *Nucleic Acids Res.* 45, 7285–7298. doi: 10.1093/nar/gkx454
- Redko, Y., De La Sierra-Gallay, I. L., and Condon, C. (2007). When all's zed and done: the structure and function of RNase Z in prokaryotes. *Nat. Rev. Microbiol.* 5, 278–286. doi: 10.1038/nrmicro1622
- Sarmiento, B. F., Leigh, J. A., and Whitman, W. B. (2011). Genetic systems for hydrogenotrophic methanogens. *Method Enzymol.* 494, 43–73. doi: 10.1016/b978-0-12-385112-3.00003-2
- Sarmiento, B. F., Mrazek, J., and Whitman, W. B. (2013). Genome-scale analysis of gene function in the hydrogenotrophic methanogenic archaeon *Methanococcus maripaludis*. *Proc. Natl. Acad. Sci. U.S.A.* 110, 4726–4731. doi: 10.1073/pnas.1220225110
- Schierling, K., Rosch, S., Rupprecht, R., Schiffer, S., and Marchfelder, A. (2002). tRNA 3' end maturation in archaea has eukaryotic features: the RNase Z from *Haloferax volcanii*. *J. Mol. Biol.* 316, 895–902. doi: 10.1006/jmbi.2001.5395
- Schiffer, S., Helm, M., Theobald-Dietrich, A., Giege, R., and Marchfelder, A. (2001). The plant tRNA 3' processing enzyme has a broad substrate spectrum. *Biochemistry* 40, 8264–8272. doi: 10.1021/bi0101953
- Schiffer, S., Rosch, S., and Marchfelder, A. (2002). Assigning a function to a conserved group of proteins: the tRNA 3'-processing enzymes. *EMBO J.* 21, 2769–2777. doi: 10.1093/emboj/21.11.2769
- Spaeth, B., Schubert, S., Lieberoth, A., Settele, F., Schuetz, S., Fischer, S., et al. (2008). Two archaeal tRNase Z enzymes: similar but different. *Arch. Microbiol.* 190, 301–308. doi: 10.1007/s00203-008-0368-4
- Spath, B., Settele, F., Schilling, O., D'angelo, I., Vogel, A., Feldmann, I., et al. (2007). Metal requirements and phosphodiesterase activity of tRNase Z enzymes. *Biochemistry* 46, 14742–14750. doi: 10.1021/bi7010459
- Stange, N., and Beier, H. (1987). A cell-free plant extract for accurate pre-tRNA processing, splicing and modification. *EMBO J.* 6, 2811–2818. doi: 10.1002/j.1460-2075.1987.tb02577.x

- Tocchini-Valentini, G. D., Fruscoloni, P., and Tocchini-Valentini, G. P. (2005). Coevolution of tRNA intron motifs and tRNA endonuclease architecture in Archaea. *Proc. Natl. Acad. Sci. U.S.A.* 102, 15418–15422. doi: 10.1073/pnas.0506750102
- Wen, T., Oussenko, I. A., Pellegrini, O., Bechhofer, D. H., and Condon, C. (2005). Ribonuclease PH plays a major role in the exonucleolytic maturation of CCA-containing tRNA precursors in *Bacillus subtilis*. *Nucleic Acids Res.* 33, 3636–3643. doi: 10.1093/nar/gki675
- Zhang, J., Li, E. H., and Olsen, G. J. (2009). Protein-coding gene promoters in *Methanocaldococcus (Methanococcus) jannaschii*. *Nucleic Acids Res.* 37, 3588–3601. doi: 10.1093/nar/gkp213
- Zheng, X., Feng, N., Li, D. F., Dong, X. Z., and Li, J. (2017). New molecular insights into an archaeal RNase J reveal a conserved processive exoribonucleolysis mechanism of the RNase J family. *Mol. Microbiol.* 106, 351–366. doi: 10.1111/mmi.13769

Conflict of Interest: The authors declare that the research was conducted in the absence of any commercial or financial relationships that could be construed as a potential conflict of interest.

Copyright © 2020 Wang, Gu, Li, Yue, Li and Dong. This is an open-access article distributed under the terms of the Creative Commons Attribution License (CC BY). The use, distribution or reproduction in other forums is permitted, provided the original author(s) and the copyright owner(s) are credited and that the original publication in this journal is cited, in accordance with accepted academic practice. No use, distribution or reproduction is permitted which does not comply with these terms.